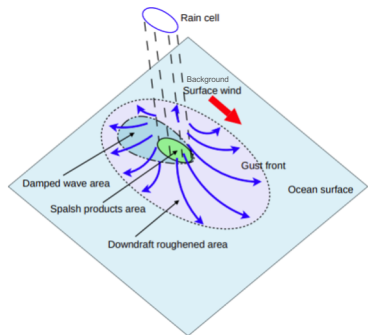


Developing a Simultaneous Wind and Rain Geophysical Model Function for OSCAT



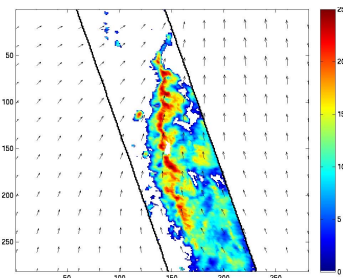
Benjamin Fogg and David G. Long

Microwave Earth Remote Sensing Lab

Brigham Young University

Provo, UT

ECMWF Winds, TRMM PR rain



This poster is presented as a sequence of slides describing our recent work and plans



Abstract

Ku-band scatterometers were originally designed to measure wind speed and direction over the ocean. Under non-raining conditions the Geophysical Model Function (GMF) captures the relationship between wind speed and direction and sigma-0. However, the presence of rain can distort the observed wind-dependent sigma-0 value, via several effects: (1) Rain drops hitting the surface modify the surface roughness both through splashing and by suppressing the wave spectrum, and (2) falling rain drops attenuate the transmitted and reflected signals and (3) introduce additional backscatter from the drops. Under these circumstances the wind-only GMF accuracy is diminished in predicting the wind speed and direction. Previously, rain specific GMFs have been created for the C-band advanced Scatterometer (ASCAT) (Owen, 2010), and QuikSCAT (Draper and Long 2004; Owen and Long 2011). The Ocean Scatterometer (OSCAT), though similar to QuikSCAT, operated at a different incidence angle and so needs a rain GMF tuned for it.

In order to create a rain GMF for OSCAT, OSCAT sigma-0, Tropical Rain Measurement Mission (TRMM) Precipitation Radar rain, and European Centre for Medium-Range Weather Forecast (ECMWF) surface winds are collocated. TRMM and ECMWF are treated as the “true” rain and wind. Along with Path Integrated Attenuation (PIA) measurements from TRMM, rain-dependent attenuation and backscatter are combined with the JPL wind GMF to derive the OSCAT rain GMF. The rain GMF is being validated using real world data using BYU’s simultaneous wind rain (SWR) algorithm. Wind estimates using SWR under rainy conditions exhibit increased accuracy relative to ECMWF compared with conventional wind-only retrieval. The results apply to both conventional resolution wind retrieval and ultra-high resolution wind retrieval.

$$\sigma^0(\text{observed}) = \sigma_{wo}(ws, wd, i) \alpha(R) + \sigma_{eff}(R) + noise$$

TRMM, ECMWF and OSCAT

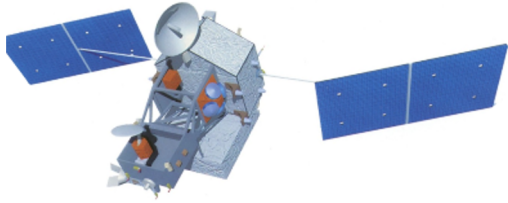


Figure 1. A model of TRMM.

Tropical Rain Measuring Mission (TRMM)

Precipitation Radar (PR) measures rainfall across the globe. Rain rate measurements are considered “truth”.

- Operating Frequency: 13.8 GHz
- Incidence Angles: range from 0°-20°
- Swath Width: 150 km

European Centre for Medium-Range Weather Forecasts (ECMWF): interpolated near-surface wind speed and direction estimates are considered “truth”

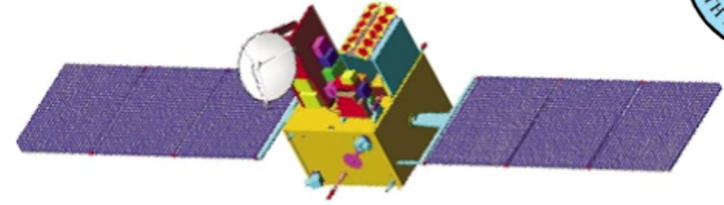


Figure 2. A model of OSCAT.

Ocean Scatterometer (OSCAT) measurements of surface backscatter (σ^0).

- Operating Frequency: 13.2 GHz
- Incidence Angles: 48° and 57°
- Swath Width: 1400 (inner) and 1836 (outer) (km)

TRMM and OSCAT Collocation

TRMM operates in a low inclination angle, while OSCAT is in a polar orbit. While this can limit the number of collocations, the TRMM orbit crosses the ASCAT orbit twice per orbit, with many of these within one hour. However for deriving the rain GMF, the temporal difference is limited to 15 mins.

ECMWF near-surface winds spatially and temporally interpolated to the individual collocation points.

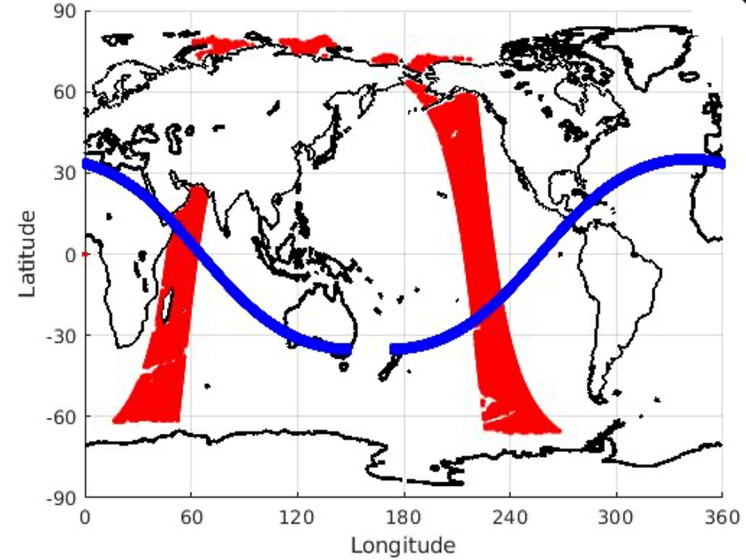


Figure 3. Coverage comparison for corresponding orbits of TRMM (blue) and OSCAT (red).

Theoretical Rain Model

$$\sigma^o = \sigma_{wo}(ws, wd, i) \alpha(R) + \sigma_{eff}(R) + noise$$

σ^o is the measured backscatter from OSCAT

σ_{wo} is the no-rain backscatter (i.e., from “background wind”) equivalent to the JPL wind-only GMF which gives sigma-0 as function of wind speed ws , relative wind direction wd , and polarization i

$\alpha(R)$ is attenuation of the surface sigma-0 due to rain

$\sigma_{eff}(R)$ is the backscatter resulting from falling rain and surface modification

The **rain GMF** are the $\alpha(R)$ and $\sigma_{eff}(R)$ functions

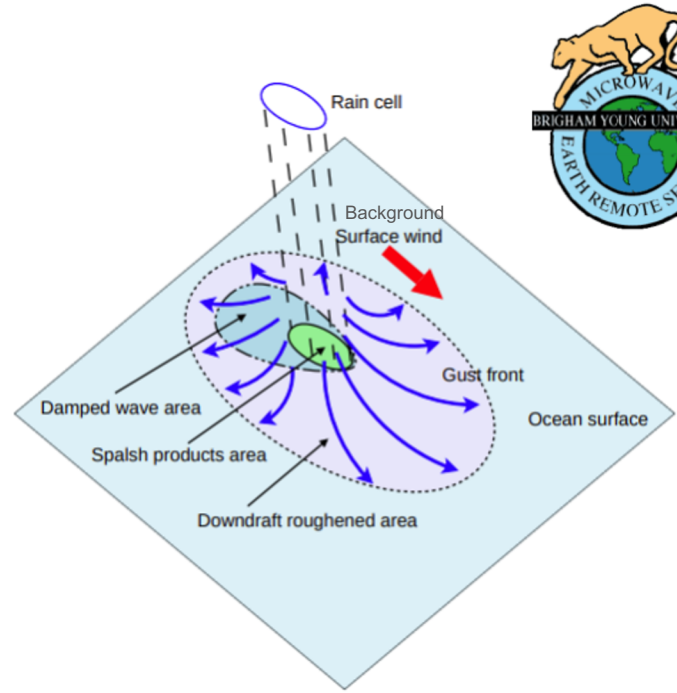


Figure 4. Illustration of how rain cells modify local winds from the “background” large scale wind flow.

Calculating $\alpha(R)$

$$PIA_{OSCAT} = \cos(\theta_{OSCAT}) / \cos(\theta_{TRMM}) PIA_{TRMM}$$

$$\alpha(R) = 10^{-PIA(R)/10}$$

Fortunately, TRMM measures the Ku-band path attenuated attenuation (PIA), albeit at a different angle than OSCAT. We adjust TRMM PR PIA's to OSCAT values and fit a simple parametric function to the measurements.

$$\alpha_{fit}(R) = ae^{bR} + ce^{dR}$$

beam	a	b	c	d
Outer	96.47	-0.06495	-95.47	-0.06468
Inner	-123	-0.05492	124	-0.05508

Table 1. Coefficients for $\alpha(R)$.

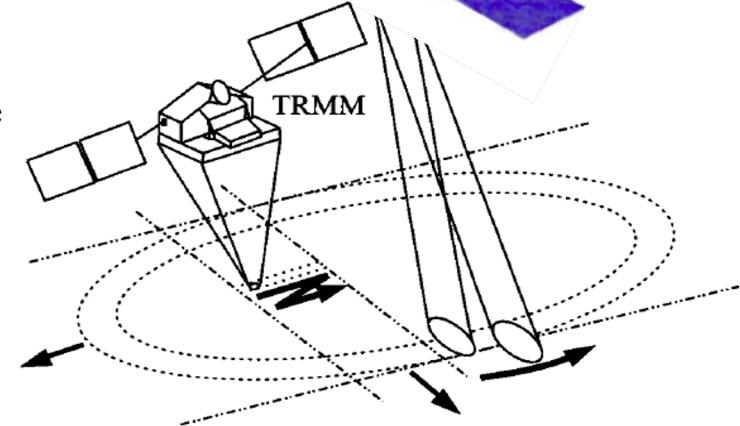


Figure 5. Comparison the swath and scanning of OSCAT and TRMM. OSCAT has two fixed incidence angles (48 and 57 deg), whereas TRMM ranges between 0 and 20 degs on either side of the nadir track.

$\alpha(R)$ Plot and Fit

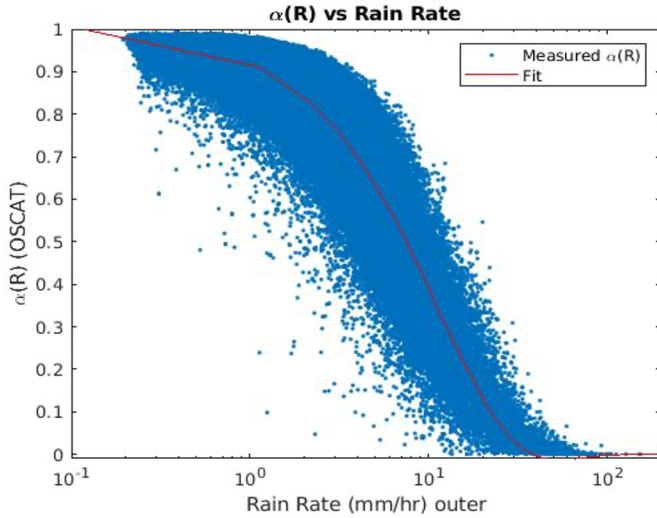


Figure 6. Outer beam calculated and fitted $\alpha(R)$ vs rain rate.

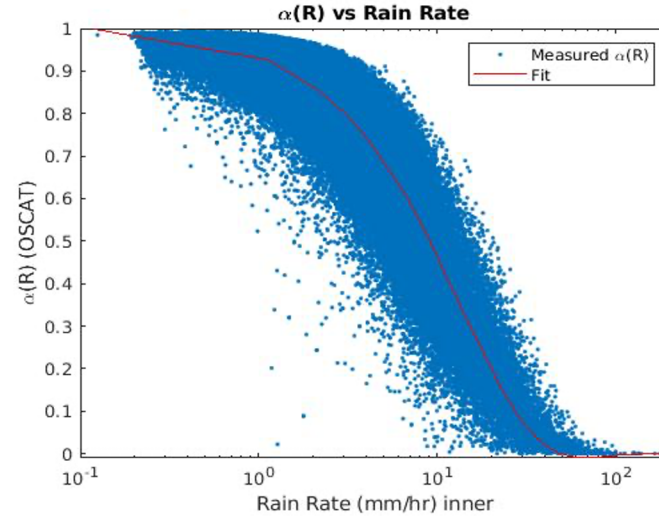


Figure 7. Inner beam calculated and fitted $\alpha(R)$ vs rain rate.

Calculating $\sigma_{\text{eff}}(R)$

$$\sigma_{\text{eff}}(R) = \sigma_{\text{meas}}^0 - \sigma_{\text{wo}}(\text{ws}, \text{wd}, \text{i}) \alpha(R) + \text{noise}$$

$$\sigma_{\text{eff_fit}}(R) = ae^{bR} + ce^{dR}$$

Two fits used for fitting $\sigma_{\text{eff}}(R)$:

- Raw measurements
- Raw measurements averaged into rain rate bins

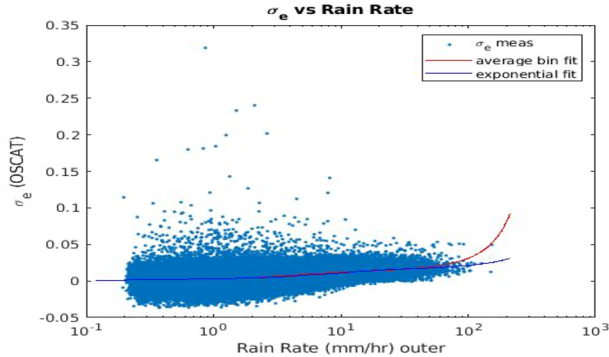


Figure 8. Outer beam calculated and fitted $\sigma_{\text{eff}}(R)$ vs Rain rate.

beam	a	b	c	d
Outer	0.01516	0.03363	-0.01412	-.1147
Inner	-0.02026	-0.11587	0.0224	0.004704

Table 2. Coefficients for σ_{eff} directly from the measurements.

beam	a	b	c	d
Outer	0.01191	0.009584	-0.01147	-0.2208
Inner	0.01982	0.0076	-0.01817	-0.2664

Table 3. Coefficients for σ_{eff} from binned averages.

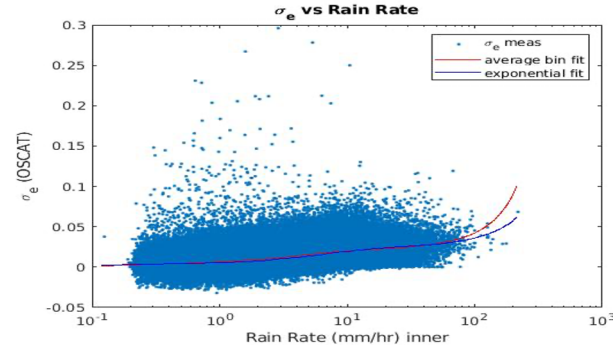


Figure 9. Inner beam calculated and fitted $\sigma_{\text{eff}}(R)$ vs rain rate.



Bibliography & References

- D.W. Draper and D.G. Long, "Evaluating the Effect of Rain on SeaWinds Scatterometer Measurements," *Journal of Geophysical Research*, Vol. 109, No. C02005, doi:10.1029/2002JC001741, 2004.
- D.W. Draper and D.G. Long, "Simultaneous Wind and Rain Retrieval Using SeaWinds Data," *IEEE Transactions on Geoscience and Remote Sensing*, Vol. 42, No. 7, pp. 1411-1423, doi:10.1109/TGRS.2004.830169, 2004.
- C. A. Mears, D. K. Smith, and F. J. Wentz, "Detecting rain with QuikSCAT," in *Proc. IGARSS, 2000*, pp. 1235–1237.
- F. Naderi, M. H. Freilich, and D. G. Long, "Spaceborne Radar Measurement of Wind Velocity Over the Ocean--An Overview of the NSCAT Scatterometer System," *Proceedings of the IEEE*, pp. 850-866, Vol. 79, No. 6, doi:10.1109/5.90163, 1991.
- M.P. Owen and D.G. Long, "Simultaneous wind and rain estimation for QuikSCAT at ultra-high resolution," *IEEE Transactions on Geoscience and Remote Sensing*, doi:10.1109/TGRS.2010.2102361, Vol. 49, No. 6, pp. 1865-1878, 2011.
- M. P. Owen, Signal Scatterometer Contamination Mitigation, Ph.D. Dissertation, Brigham Young University, Provo, Utah, 2010.
- L. Ricciardulli & F. Wentz, "A Scatterometer Geophysical Model Function for Climate-Quality Winds: QuikSCAT Ku-2011," *Journal of Atmospheric and Oceanic Technology*, Vol. 32, No. 150904131243002. doi:10.1175/JTECH-D-15-0008.1, 2015.
- F. Ulaby and D.G. Long, *Microwave Radar and Radiometric Remote Sensing*, ISBN: 978-0-472- 11935-6, University of Michigan Press, Ann Arbor, Michigan, 2013.
- F.J. Wentz and D.K. Smith, "A model function for the ocean-normalized radar cross section at 14 GHz derived from NSCAT observations," *Journal of Geophysical Research*, 104 (C5), 11499– 11514, doi:10.1029/98JC02148, 1999.